When Tissue Speaks: Vibroacoustic Monitoring of Tissue Response during Electrosurgery

Nazila Esmaeili[1] [0000-0001-9741-9788], Robin Urrutia[2,3] [0009-0003-9430-3474], Diego Espejo[2,4] [0000-0001-8083-538X], Axel Boese[5] [0000-0002-5874-7145], Philipp Horvath[6] [0009-0003-6249-5766], Christian Hansen[2,3] [0009-0000-1530-4291], Jannis Hagenah[1,7] [0000-0002-3320-0186], and Alfredo Illanes[2,3] [0000-0002-0118-0483]

[1] Center for Digital Surgery, Department of General, Visceral and Pediatric Surgery, University Medical Center Göttingen, 37075 Göttingen, Germany.
nazila.esmaeili@med.uni-goettingen.de
[2] Otto von Guericke University Magdeburg, Faculty of Computer Science, Universitätsplatz 2, 39106 Magdeburg, Germany.
[3] Research Campus STIMULATE, Otto-Hahn-Str. 2, 39106 Magdeburg, Germany.
[4] Innovation Center Computer-Assisted Surgery (ICCAS), Faculty of Medicine, Leipzig University, Semmelweisstraße 14, 04103 Leipzig, Germany.
[5] Otto von Guericke University Magdeburg, Innovation Laboratory for Image Guided Therapy, Leipziger Str. 44, 39120 Magdeburg, Germany.
[6] Department of General, Visceral and Pediatric Surgery, University Medical Center Göttingen, 37075 Göttingen, Germany.
[7] Fraunhofer Research Institution for Individualized and Cell-based Medical Engineering (IMTE), 23562 Lübeck, Germany.

Abstract. Electrosurgical coagulation is widely used in laparoscopic surgery; however, intraoperative assessment of tissue response remains indirect and largely reliant on visual cues, increasing the risk of insufficient coagulation or excessive thermal damage. In this work, we investigate vibroacoustic (VA) sensing as a non-invasive modality for monitoring electrosurgical coagulation. VA sensing captures structure-borne mechanical vibrations generated at the tool-tissue interaction point without requiring modifications to standard surgical instruments or workflows. Using a bipolar electrosurgical setup, VA signals were acquired under two complementary scenarios: prolonged coagulation of ex vivo porcine liver tissue to analyze temporal signal evolution, and coagulation of ex vivo porcine liver, muscle, and fat to investigate tissue-specific responses. The signals were analyzed using time- and time-frequency-domain signal processing methods. Results show that VA signals evolve systematically throughout coagulation, revealing distinct phases up to carbonization. In addition, tissue-specific analyses demonstrate reproducible differences in temporal dynamics and spectral content, enabling clear separation of tissue types in a non-linear embedding space. These findings indicate that VA sensing captures reproducible state-dependent and tissue-specific characteristics during electrosurgical energy delivery, highlighting its potential to address the clinical challenge of perceiving and controlling tissue response during electrosurgery.

Keywords: Vibroacoustic sensing · Tissue monitoring · Electrosurgery.

1 Introduction

Electrosurgery is an integral component of laparoscopic surgery, where conventional monopolar and bipolar modalities remain the most used tools for tissue dissection, coagulation, and vessel sealing [12, 1]. Effective electrosurgical treatment, while minimizing the risk of lateral thermal spread, depends on the surgeon's ability to accurately perceive and control tissue response during energy delivery [5]. However, this remains challenging in laparoscopic settings. Tissue response can only be inferred from indirect visual cues, such as surface color changes and the release of water vapor, which do not reliably reflect subsurface tissue state. Visual assessment is further constrained by the camera-mediated field of view, where parts of the instruments and surrounding tissues may lie outside the visible area, and by electrosurgical smoke that can degrade image quality. Moreover, accurate interpretation of these cues depends on the surgeon's experience and understanding of electrosurgical principles, which often require dedicated training. Together, these limitations increase the risk of under-treatment, resulting in insufficient tissue coaptation, incomplete coagulation, and persistent bleeding, or over-treatment, leading to carbonization and increased lateral thermal spread [13, 9]. To mitigate these risks, advanced systems such as LigaSure™, EnSeal™, Plasma Kinetic Gyrus™, and ultrasonic technologies have been shown to reduce lateral thermal spread, operative time, and intraoperative blood loss. However, their clinical integration remains limited; therefore, conventional electrosurgical devices continue to be widely used due to their familiarity, cost-effectiveness, and adaptability across diverse surgical scenarios [12]. Modern electrosurgical units commonly incorporate impedance-based feedback mechanisms that modulate energy delivery according to tissue electrical properties. However, these systems control electrical measurements and do not provide direct information about the local tissue state or the progression of thermal effects. Moreover, this feedback is not explicitly conveyed to the surgeon during the procedure. Consequently, perceiving and controlling tissue response during electrosurgery remains challenging in current setting [20, 2, 16].

Electrosurgical tissue effects are not purely electrical or thermal phenomena. Tissue heating induces a sequence of thermally driven biological and structural changes that are accompanied by mechanical processes, including vibrations generated at the tool-tissue interaction point [3, 4]. These mechanically induced responses represent a natural but largely underexplored source of information that can provide insight into tissue state during electrosurgery. Vibroacoustic (VA) sensing enables access to this structure-borne vibration information. By placing a sensor on the proximal part of the surgical instrument, vibrations generated at the tool-tissue interaction that propagate along the instrument shaft can be acquired outside the body. This enables passive sensing without the need for active components inside the body, without modifying standard instruments, and without interfering with existing surgical workflows. This modality provides simple and non-invasive access to a rich source of information with high dynamical range. The feasibility of VA sensing has been demonstrated in various applications, including pedicle screw loosening and breach detection during spinal pedicle drilling [18, 10], tissue characterization in needle-based procedures [17, 8], and audification of laparoscopic surgical tasks [6]. In parallel, airborne acoustic signals have also been explored in laparoscopic procedures, where microphones capture sound generated during surgical activity in experimental setups. These studies have demonstrated that airborne audio contains informative features for perception enhancement and high-level classification tasks, including differentiation of cutting and coagulation modes [14, 15]. However, they rely on sound transmitted through the air and do not provide direct access to structure-borne vibrations at the tool-tissue interaction point.

As the ability to directly monitor tissue response during electrosurgical energy delivery through structure-borne vibrations remains largely unexplored, this work investigates VA sensing as a novel modality for monitoring electrosurgical coagulation by capturing state-dependent and tissue-specific responses during energy delivery. The main contributions are:

- We introduce VA sensing as a non-invasive and tool-agnostic modality for capturing state-dependent and tissue-specific responses during electrosurgical energy delivery.
- We demonstrate that VA signals evolve systematically throughout the prolonged electrosurgical coagulation process, revealing distinct phases up to tissue carbonization.
- We analyze tissue-specific VA responses during electrosurgical coagulation and show that different tissue types exhibit distinct signatures, enabling discrimination based on thermal response.

2 Method

In accordance with the stated contributions, the experimental setup and analysis framework were designed to investigate VA behavior during electrosurgical coagulation using two complementary acquisition scenarios, where all coagulations were performed by an experienced surgeon: scenario I addressing the evolution of VA dynamics during prolonged coagulation up to carbonization, and scenario II examining tissue-specific responses under comparable conditions. The signal processing strategy enabled structured analysis of temporal evolution and inter-tissue variability in VA signals and was implemented in MATLAB R2024b and Python. The data and code supporting the findings of this study are available at https://gitlab.gwdg.de/cds/va-electrosurgery.

2.1 Experimental Setup and Data Acquisition

All experiments used a unified setup and predefined protocol to record VA signals during electrosurgical coagulation.

A schematic overview of the experimental setup is shown in Fig. 1. Electrosurgical energy was delivered using a high-frequency electrosurgical unit (VIO® 300D, Erbe Elektromedizin GmbH, Tübingen, Germany), which generates and

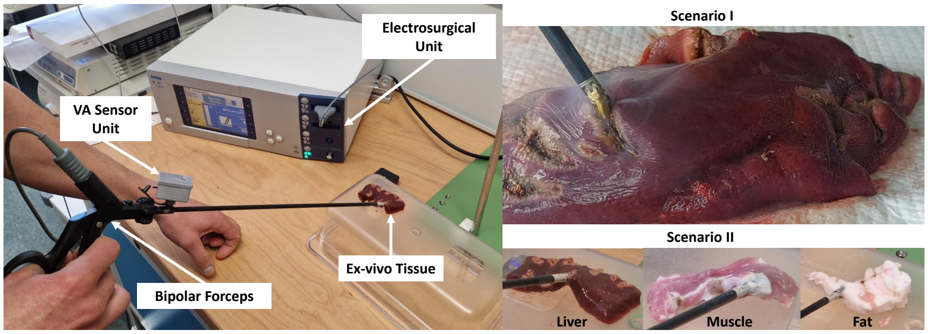

Fig. 1. The overview of experimental setup with the experiments of scenario I and II.

modulates electrical current for different surgical effects. Bipolar energy was applied using a standard rotating bipolar grasping forceps (RoBi®, KARL STORZ, Tuttlingen, Germany). VA signals were acquired using a VA sensing system (SURAG Medical GmbH, Leipzig, Germany). The add-on sensor was mounted proximally on the bipolar forceps using the instrument's existing Luer-lock connection, without any modification of the surgical tool. VA data were transmitted wirelessly in real-time to a laptop. Dedicated software enabled signal acquisition, optional real-time audification, and storage for offline analysis. VA signals were recorded at a sampling frequency of 44400 Hz. In addition, an external video recording of the entire experiment was acquired.

A standardized acquisition protocol was applied in all experiments. Each trial began with the instrument placed on the table while VA recordings captured background noise for 5–10 s. The surgeon then picked up the instrument, and a reproducible synchronization event was generated by three taps on the instrument shaft, producing distinct peaks visible in both VA and video modalities. The surgeon subsequently grasped the tissue and performed coagulation. After task completion, the instrument was placed back on the table and all recordings were stopped.

In scenario I, a whole ex vivo porcine liver was used. This scenario comprised a total of 15 VA recordings. In each trial, the surgeon performed coagulation continuously on the tissue until visual cues indicated complete carbonization. In scenario II, three ex vivo porcine tissue types (liver, muscle, and fat) were investigated. Samples were prepared with comparable dimensions ($\approx 10 \times 3 \times 1$ cm) to ensure experimental consistency. For each tissue type, 10 VA recordings were obtained (30 total). This design enabled direct comparison of tissue-specific VA characteristics while minimizing geometric and procedural variability.

For all experiments, the recorded video and its audio track were used to synchronize video and VA recordings. The start and end of each coagulation event were manually annotated in the synchronized video data, and the corresponding VA signal segments were extracted using these annotations for subsequent analysis.

2.2 Vibroacoustic Data Analysis

Figure 2 illustrates the overall VA signal analysis strategy. The acquired signals were divided into two datasets corresponding to scenarios I and II. All recordings underwent a common processing pipeline, followed by specific analyses for each scenario.

The common signal processing pipeline began with pre-processing of each raw VA segment. First, the DC component was removed. Background noise was then attenuated using spectral gating by computing the spectrogram and estimating a frequency-dependent noise threshold. A binary mask was constructed to suppress spectral components below this threshold to provide the denoised time-domain VA signal. The resulting signal was used for subsequent analysis in scenario II. In the final step of this pipeline, a time-pseudo-frequency representation was computed using the Continuous Wavelet Transform (CWT) with a Morse mother wavelet. The resulting CWT matrix captures VA energy over time and pseudo frequency and forms the basis for the analyses in scenario I and II.

For scenario I, the CWT spectra were first visually inspected to identify frequency bands showing consistent dynamical changes during prolonged coagulation. For each selected band, an instantaneous band-energy contribution indicator $C(t)$ was computed. At each time point, total spectral energy $E_T(t)$ and band-specific energy $E_B(t)$ were calculated from the CWT matrix. The relative contribution was then defined as $C(t) = (E_B(t) \div E_T(t)) \times 100$. Repeating this procedure over time yielded a band-specific time-series indicator reflecting the relative energy contribution throughout coagulation. These indicators were analyzed to evaluate changes in VA dynamics during prolonged coagulation.

In scenario II, four indicators were extracted to characterize tissue-specific VA behavior. Two indicators were derived from the pre-processed time-domain VA signal. Indicator 1 captured energy evolution using a homomorphic envelope, followed by applying a low-pass filter to isolate the slow-varying amplitude component, yielding a time-series reflecting coagulation dynamics. Indicator 2 quantified transient activity by detecting peaks in the signal and applying a moving average filter to obtain a smoothed peak density time-series. Two remaining indicators were computed from the CWT representation. Indicator 3 was obtained by first scaling the CWT matrix to $[0, 1]$ and then averaging over time, emphasizing relative frequency structure independent of absolute energy. Indicator 4 was computed by averaging the original CWT matrix over time, providing information about the spectral energy distribution. In the final stage of data analysis in scenario II, the four indicator vectors from each trial were jointly embedded using Uniform Manifold Approximation and Projection (UMAP) as a descriptive visualization method, without label information [7]. UMAP was configured to generate a compact low-dimensional representation that preserves local structure in the data, using 3 nearest neighbors, a minimum distance of 0.1, and *Euclidean* metric. The resulting coordinates were then used as input to a k-Nearest Neighbors (kNN) classifier to assess supervised local label consistency and visualize class separation [21].

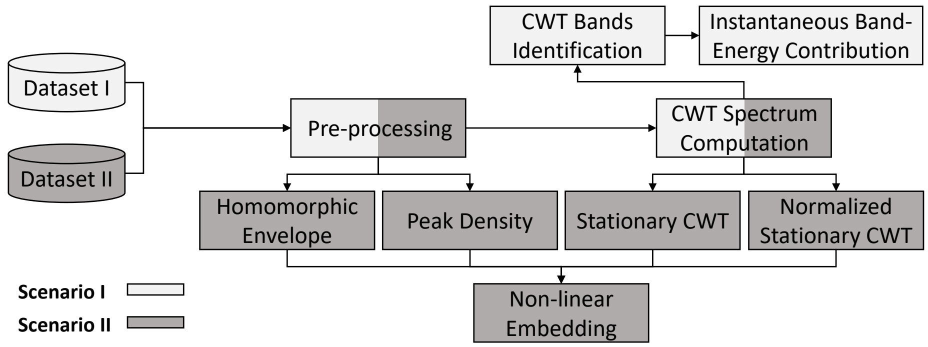

Fig. 2. The block diagram of VA data analysis for scenario I and II.

3 Results and Discussion

Figure 3 presents the results of scenario I, illustrating the temporal evolution of VA signals during prolonged liver coagulation. Fig. 3(a) shows the CWT time-pseudo-frequency spectrum of a representative VA signal from the onset of electrosurgical activation to visually confirmed completion of tissue carbonization. The spectrum reveals systematic dynamical changes across three pseudo-frequency regions: low-frequency (LF, 1–200 Hz), mid-frequency (MF, 250–3000 Hz), and high-frequency (HF, 5000–12000 Hz). Fig. 3(b–d) show the instantaneous band-energy contribution indicator (%) of the identified LF, MF, and HF bands. Joint inspection of these indicators and the CWT spectrum identifies two transition points (approximately 2.3 s and 7.5 s; marked red lines), dividing the signal into three phases (Ph) with distinct band dynamics. Ph1 is characterized by dominant LF activity and low HF contribution. In Ph2, HF increases markedly with strong LF attenuation while MF remains consistently active. In Ph3, HF decreases, LF increases again, and MF reduces relative to Ph2.

To evaluate whether these observations generalize across all 15 recordings in a quantitative way, each trial was manually and independently segmented into three phases based on the transition points observed in its CWT spectrum and band-energy contribution indicators. For each phase, the CWT spectrum was averaged over time to obtain a phase-specific stationary spectrum. The spectral energy contribution of the LF, MF, and HF bands was then computed as the ratio between band-specific energy and total spectral energy (%). Fig. 3(e) presents boxplots of these band-energy contributions, confirming consistent phase-dependent dynamics across trials, including HF increase in Ph2, dominant MF activity peaking in Ph2, and reduced LF contribution during Ph2. Additionally, total spectral energy within each phase was computed by integrating the segmented CWT spectrum over time and frequency. The boxplots in Fig. 3(f) demonstrate comparable total spectral energy levels in Ph1 and 2, whereas Ph3 shows a consistent reduction in overall VA energy, indicating a distinct change in signal behavior.

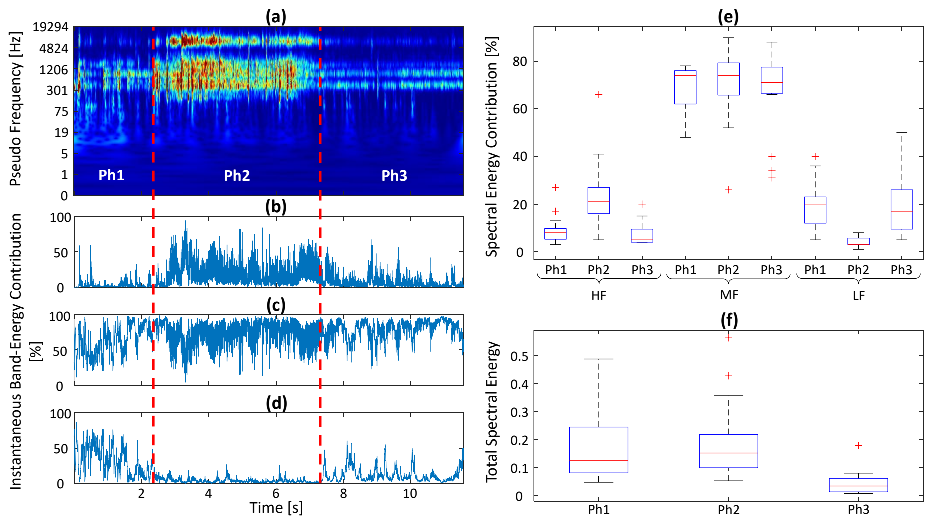

Fig. 3. Results of scenario I. (a): CWT spectrum, Instantaneous band-energy contribution indicator for (b): HF band, (c): MF band, (d): LF band, (e): Boxplot of spectral energy contribution, and (f): Boxplot of total spectral energy.

These findings confirm that VA signals evolve in a structured and reproducible manner during electrosurgical coagulation, exhibiting consistent transitions in band-specific dynamics that delineate distinct phases up to tissue carbonization. The observed phase-dependent changes appear consistent with thermally induced tissue transformations during electrosurgery, where heating can progress from early fluid-related effects to desiccation and protein coagulation and, with continued energy delivery, carbonization [11, 19, 3]. In Ph1, the clear transients reflect mechanically unstable events that could be associated with rapid water vaporization in highly hydrated tissue, such as liver. The marked increase in MF and HF contributions in Ph2 could correspond to tissue desiccation and coagulation, where progressive drying and structural stiffening alter the interaction dynamics and redistribute spectral energy. Finally, Ph3 aligns with direct visual inspection of the recorded video data confirming the onset of carbonization. This phase is accompanied by reduced total VA energy and altered band dynamics, indicating a distinct interaction regime once the tissue becomes carbonized.

Fig. 4 presents the results of scenario II based on all 30 VA signals acquired during electrosurgical coagulation of three tissue types. Each matrix corresponds to one indicator and consists of vectors from repeated trials per tissue, enabling global qualitative assessment of tissue-specific behavior. Indicator 1 (Fig. 4(a)) shows a rapid rise followed by fast decay for liver, indicating a short temporal response with most variation occurring early in coagulation. Muscle and fat show more gradual changes with longer-lasting signal intensity and slower decay. This suggests faster VA dynamics in liver compared to the more prolonged responses

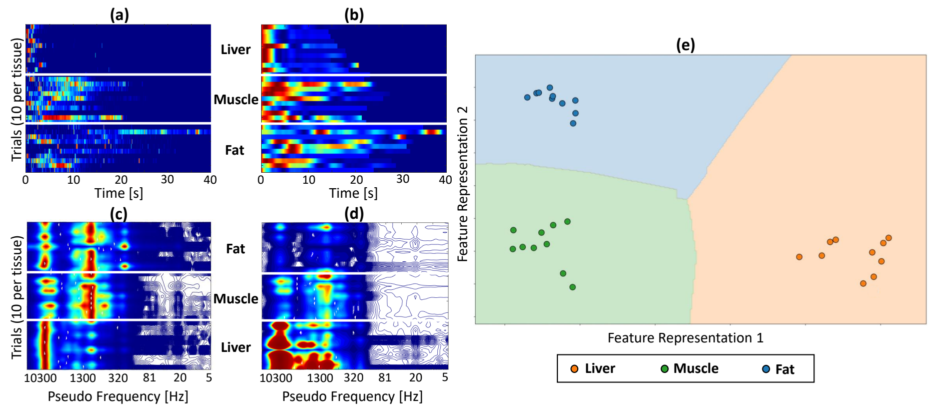

Fig. 4. Results of scenario II. (a): Indicator 1 (homomorphic envelop), (b): Indicator 2 (peak density), (c): Indicator 3 (normalized stationary CWT), (d): Indicator 4 (stationary CWT), and (e): UMAP visualization with kNN decision boundaries.

observed in muscle and fat. Indicator 2 (Fig. 4(b)) confirms this behavior. Liver shows concentrated transient activity early in coagulation, whereas muscle and fat display more distributed activity over time. These indicators reveal distinct temporal characteristics across tissues, with faster dynamics for liver, intermediate for muscle, and slower for fat. Indicator 3 (Fig. 4(c)) shows a narrow-band response dominated by a single frequency component for liver, indicating a relatively homogeneous vibration pattern. Muscle and fat exhibit broader spectra with mainly two dominant frequency components, indicating more complex vibration behavior, while fat shows slightly higher dominant frequency content than muscle. Indicator 4 (Fig. 4(d)) further reveals higher overall energy levels for liver compared to muscle and fat which is consistent with the faster and more concentrated signal activity observed in the time-domain indicators.

To further assess tissue differentiation, Fig. 4(e) shows the UMAP embedding of all indicators along with the corresponding kNN decision boundaries. The embedding reveals three compact, well-separated clusters corresponding to the three tissues. Clear decision boundaries without overlap indicate complete separability in the learned latent space, demonstrating that the extracted VA indicators enable robust tissue differentiation during electrosurgical coagulation. These results demonstrate that VA responses exhibit distinct and consistent tissue-specific patterns, reflecting reproducible signal characteristics of the tool-tissue interaction during electrosurgical coagulation that enable discrimination between tissue types based on their VA signatures.

4 Conclusion

In this study, we introduced VA sensing as a non-invasive, tool-agnostic modality for capturing state-dependent and tissue-specific responses during electrosurgry. We demonstrated that VA signals evolve systematically during prolonged coagulation, exhibiting reproducible phase transitions as response to tissue thermal changes up to carbonization. Furthermore, different tissue types generated consistent and distinct VA signatures, enabling discrimination based on their thermal response. Together, these findings position VA sensing as a promising approach to address the clinical challenge of perceiving and controlling tissue response during electrosurgery by providing objective information on tissue state progression and interaction dynamics. Although the observed VA phases align with expected thermally induced tissue changes, the biological interpretation is based on indirect evidence and requires validation. Future work will address this limitation through controlled thermal correlation studies, followed by extension to in vivo settings and evaluation of real-time clinical integration.

Acknowledgments. The authors would like to thank KARL STORZ SE & Co. KG (Tuttlingen, Germany) for providing the bipolar laparoscopic instrument and SURAG Medical GmbH (Leipzig, Germany) for providing the VA sensing system.

Disclosure of Interests. Nazila Esmaeili, Axel Boese and Alfredo Illanes are shareholders of SURAG Medical GmbH.

References

1. Abi Antoun, M., Etrusco, A., Chiantera, V., Laganà, A.S., Feghali, E., Khazzaka, A., Stabile, G., Della Corte, L., Dellino, M., Sleiman, Z.: Outcomes of conventional and advanced energy devices in laparoscopic surgery: a systematic review. Minimally Invasive Therapy & Allied Technologies **33**(1), 1–12 (2024)
2. Bao, C., Mazumder, S.K.: Output power computation and adaptation strategy of an electrosurgery inverter for reduced collateral tissue damage. IEEE Transactions on biomedical engineering **70**(6), 1729–1740 (2022)
3. Bianchi, L., Cavarzan, F., Ciampitti, L., Cremonesi, M., Grilli, F., Saccomandi, P.: Thermophysical and mechanical properties of biological tissues as a function of temperature: a systematic literature review. International Journal of Hyperthermia **39**(1), 297–340 (2022)
4. El-Sayed, M.M., Saridogan, E.: Principles and safe use of electrosurgery in minimally invasive surgery. Gynecology and Pelvic Medicine **4**, 6 (2021)
5. El-Sayed, S., Saridogan, E., El-Sayed, M.: Complications of electrosurgery: mechanisms and prevention strategies. Facts, Views & Vision in ObGyn **16**(4), 473 (2024)
6. Esmaeili, N., Sühn, T., Illanes, A., Fischerauer, S., Boese, A., Bußhoff, J., Datta, R.: Laparoscopic surgery augmentation through vibro-acoustic sensing of instrument-tissue interactions. Current Directions in Biomedical Engineering **9**(1) (2023)
7. Healy, J., McInnes, L.: Uniform manifold approximation and projection. Nature Reviews Methods Primers **4**(1), 82 (2024)
8. Heryan, K., Serwatka, W., Rzepka, D., Fuentealba, P., Friebe, M.: Exploratory analysis and framework for tissue classification based on vibroacoustic signals from needle–tissue interaction. International Journal of Computer Assisted Radiology and Surgery **20**(9), 1795–1806 (2025)

9. Lin, X., Fan, Q., Li, R., Chen, R., Yang, Z., Li, Y.: Enhancing laparoscopic visibility: efficient surgical smoke clearance innovatively using nebulization technology. BioMedical Engineering OnLine **24**(1), 65 (2025)
10. Massalimova, A., Timmermans, M., Cavalcanti, N., Suter, D., Seibold, M., Carrillo, F., Laux, C.J., Sutter, R., Farshad, M., Denis, K., et al.: Automatic breach detection during spine pedicle drilling based on vibroacoustic sensing. Artificial Intelligence in Medicine **144**, 102641 (2023)
11. Massarweh, N.N., Cosgriff, N., Slakey, D.P.: Electrosurgery: history, principles, and current and future uses. Journal of the American College of Surgeons **202**(3), 520–530 (2006)
12. Meneses Alves, T., Ferreira De Castro, L., Tomé, A., Ferreira, H.: Applications of different energy devices in laparoscopic and robotic gynecological surgery: a systematic review. Archives of gynecology and obstetrics **312**(3), 691–719 (2025)
13. Messenger, D., Carter, F., Noble, E., Francis, N.: Electrosurgery and energized dissection. Surgery (oxford) **38**(3), 133–138 (2020)
14. Ostler, D., Seibold, M., Fuchtmann, J., Samm, N., Feussner, H., Wilhelm, D., Navab, N.: Acoustic signal analysis of instrument–tissue interaction for minimally invasive interventions. International Journal of Computer Assisted Radiology and Surgery **15**(5), 771–779 (2020)
15. Ostler-Mildner, D., Wegener, L., Fuchtmann, J., Feussner, H., Wilhelm, D., Navab, N.: The sound of surgery-development of an acoustic trocar system enabling laparoscopic sound analysis. International Journal of Computer Assisted Radiology and Surgery **19**(12), 2389–2397 (2024)
16. Rafiq, M.M., Ibeas, A., Ullah, N.: Expert knowledge-based peak current mode control of electrosurgical generators for improved output power regulation. Journal of Electrical Bioimpedance **14**(1), 32 (2023)
17. Sayahkarajy, M., Römer, F., Witte, H.: Vibroacoustic detection of inclusions in elastomer tissue phantom using mlp: A proof-of-concept. Journal of the mechanical behavior of biomedical materials p. 107279 (2025)
18. Seibold, M., Sigrist, B., Götschi, T., Widmer, J., Hodel, S., Farshad, M., Navab, N., Fürnstahl, P., Laux, C.J.: A new sensing paradigm for the vibroacoustic detection of pedicle screw loosening. Medical & Biological Engineering & Computing **63**(4), 1001–1011 (2025)
19. Taheri, A., Mansoori, P., Sandoval, L.F., Feldman, S.R., Pearce, D., Williford, P.M.: Electrosurgery: part i. basics and principles. Journal of the American Academy of Dermatology **70**(4), 591–e1 (2014)
20. Tomov, V., Tabakov, S., Panov, G.: Modern advances in energy based electrosurgical devices. Electrotech Electron (E+ E) **52** (2017)
21. Wu, Y., Ianakiev, K., Govindaraju, V.: Improved k-nearest neighbor classification. Pattern recognition **35**(10), 2311–2318 (2002)